Video Article

A Preclinical Mouse Model of Osteosarcoma to Define the Extracellular Vesicle-mediated Communication Between Tumor and Mesenchymal Stem Cells

Tonny Lagerweij*[1], Maria Pérez-Lanzón*[2], S. Rubina Baglio[2]

[1]Neuro-oncology Research Group, VU Medical Center

[2]Exosomes Research Group, Department of Pathology, VU Medical Center

*These authors contributed equally

Correspondence to: S. Rubina Baglio at s.baglio@vumc.nl

URL: https://www.jove.com/video/56932
DOI: doi:10.3791/56932

Keywords: Cancer Research, Issue 135, Orthotopic cancer mouse model, mesenchymal stem cells, extracellular vesicles, tumor microenvironment, metastasis, osteosarcoma

Date Published: 5/6/2018

Citation: Lagerweij, T., Pérez-Lanzón, M., Baglio, S.R. A Preclinical Mouse Model of Osteosarcoma to Define the Extracellular Vesicle-mediated Communication Between Tumor and Mesenchymal Stem Cells. *J. Vis. Exp.* (135), e56932, doi:10.3791/56932 (2018).

Abstract

Within the tumor microenvironment, resident or recruited mesenchymal stem cells (MSCs) contribute to malignant progression in multiple cancer types. Under the influence of specific environmental signals, these adult stem cells can release paracrine mediators leading to accelerated tumor growth and metastasis. Defining the crosstalk between tumor and MSCs is of primary importance to understand the mechanisms underlying cancer progression and identify novel targets for therapeutic intervention.

Cancer cells produce high amounts of extracellular vesicles (EVs), which can profoundly affect the behavior of target cells in the tumor microenvironment or at distant sites. Tumor EVs enclose functional biomolecules, including inflammatory RNAs and (onco)proteins, that can educate stromal cells to enhance the metastatic behavior of cancer cells or to participate in the pre-metastatic niche formation. In this article, we describe the development of a preclinical cancer mouse model that enables specific evaluation of the EV-mediated crosstalk between tumor and mesenchymal stem cells. First, we describe the purification and characterization of tumor-secreted EVs and the assessment of the EV internalization by MSCs. We then make use of a multiplex bead-based immunoassay to evaluate the alteration of the MSC cytokine expression profile induced by cancer EVs. Finally, we illustrate the generation of a bioluminescent orthotopic xenograft mouse model of osteosarcoma that recapitulates the tumor-MSC interaction, and show the contribution of EV-educated MSCs to tumor growth and metastasis formation.

Our model provides the opportunity to define how cancer EVs shape a tumor-supporting environment, and to evaluate whether blockade of the EV-mediated communication between tumor and MSCs prevents cancer progression.

Video Link

The video component of this article can be found at https://www.jove.com/video/56932/

Introduction

The tumor microenvironment actively participates in most, if not all, aspects of tumorigenesis and cancer progression, including metastasis formation and the development of resistance to therapeutics[1]. This stresses the need for preclinical orthotopic cancer mouse models that allow dissection of the complex tumor-stroma interactions occurring in the tumor niche.

Among the many cellular components of the tumor microenvironment, mesenchymal stem cells (MSCs) strongly contribute to cancer progression in multiple cancer types such as breast cancer, prostate cancer, brain tumors, multiple myeloma, and osteosarcoma[2,3,4,5,6,7]. MSCs are multipotent stem cells that reside in various adult and fetal tissues, including bone marrow, adipose tissue, placenta, umbilical cord blood, and others[8,9]. In response to cancer-generated inflammatory signals, MSCs migrate towards tumor sites, incorporate into the tumor microenvironment and ultimately differentiate into cancer-supporting cells[10]. These cancer-associated MSCs provide essential factors (*i.e.,* growth factors, chemokines, cytokines, and immunosuppressive mediators) for tumor progression acting both on tumor cells and on the surrounding stroma[2,3,11,12,13]. While the tumor-promoting effects of cancer-associated MSCs have been investigated in numerous cancer models, the mechanisms by which tumor cells reprogram MSCs to shape a cancer-promoting niche are poorly understood. Here we describe the generation of an orthotopic xenograft model that specifically allows the study of the pro-tumorigenic interaction between bone cancer cells and MSCs via extracellular vesicles (EVs).

EVs are crucial mediators of intercellular communication between tumor and stromal cells[14]. EVs carry functional biomolecules of the cell of origin, including proteins, lipids, and regulatory RNAs. Once released in the extracellular space, these vesicles can be taken up by surrounding cells or carried to distant sites via the blood or the lymphatic circulation, and can profoundly influence target cell behavior.[15,16,17] For instance,

uptake of cancer EVs by stromal fibroblasts may result in myofibroblast differentiation supporting angiogenesis and accelerating tumor growth *in vivo*[18,19], internalization by endothelial cells can stimulate tumor angiogenesis and increase vascular permeability[16,20], and interaction with immune cells might lead to suppression of the antitumor immune response[21].

We recently demonstrated, using a bioluminescent orthotopic xenograft mouse model of osteosarcoma, that tumor cells release high amounts of EVs that prompt MSCs to acquire a pro-tumorigenic and pro-metastatic phenotype. This effect is due to a dramatic change in the MSC cytokine expression profile (referred to as "MSC education"), and can be prevented by the administration of a therapeutic interleukin-6 receptor (IL-6R) antibody[7]. Our work demonstrated that cancer EVs are crucial modulators of MSC behavior, thus providing a rationale for microenvironment-targeted approaches to halt osteosarcoma progression. Herein, we describe a step-by-step protocol to investigate the EV-mediated tumor-MSC interaction *in vivo*. This model is intended to: 1) specifically define the cancer EV-induced alterations of MSC behavior in the tumor microenvironment, 2) evaluate how this interaction contributes to bone tumor growth and metastasis formation, and 3) study whether interfering with the EV-mediated crosstalk *in vivo* prevents cancer progression.

Protocol

Human adipose tissues for mesenchymal stem cell isolation were obtained from the department of Plastic Surgery of the Tergooi Hospital (Hilversum, Netherlands) after approval by the Institutional Ethical Committee and written informed consent. GFP-positive adipose MSCs were obtained from the Department of Medical and Surgical Sciences for Children and Adults (University of Modena and Reggio Emilia).

Animal experiments were performed in accordance with the Dutch law on animal experimentation, and the protocol was approved by the committee on animal experimentation of the VU University medical center, Amsterdam, Netherlands.

1. Isolation of Tumor-Secreted Extracellular Vesicles.

1. Prepare EV-depleted Fetal Bovine Serum (FBS) by centrifuging FBS at 70,000 x g overnight (16 hours), no brake, at 4 °C using an ultra-swinging bucket rotor (expect 1 h for deceleration). Carefully collect the supernatant (EV-depleted FBS) without disturbing the pellet. Filter the EV-depleted FBS with a 0.22 µm filter.
2. Prepare EV-depleted culture medium by supplementing Iscove's Modified Dulbecco's Medium (IMDM) with 100 U/mL penicillin, 100 µg/mL streptomycin, 2 mM glutamine (1x P/S/G) and 5% EV-depleted FBS.
3. Seed 3 x 10^6 143B cells in 175 cm^2 flasks and culture them in EV-depleted culture medium in an incubator at 37 °C and 5% CO_2. When the cells are 80 - 90% confluent (typically after 36 h to 48 h), collect the supernatant from 8x 175 cm^2 flasks (28 mL/flask) for EV-isolation.
4. Pre-clear the cell supernatant to remove cells and cell debris by differential centrifugation (centrifuging the supernatant of the previous spin each time) according to the following protocol:
    1. Centrifuge the supernatant twice at 500 x g for 10 min.
    2. Centrifuge the supernatant twice at 2000 x g for 15 min.
    3. Centrifuge the supernatant twice at 10,000 x g for 30 min.
    4. Perform all centrifugations at 4 °C with maximum acceleration and deceleration speed settings. After each step, carefully collect the EV-containing supernatant, leaving about 1 mL behind. Proceed immediately to step 1.5 or store the pre-cleared conditioned medium at -80 °C until EV isolation.
5. Isolate EVs by centrifuging the pre-cleared conditioned medium once at 70,000 x g for 1 h, slow brake, at 4 °C in ultra-centrifuge tubes (final volume 38.5 mL/tube) using an ultra-swinging bucket rotor.
6. Carefully remove the supernatant, leaving about 1 mL behind, resuspend the EV-containing pellets in the remaining volume, pool them all in one ultracentrifuge tube, and add phosphate-buffered saline (PBS) until complete tube filling (final volume 38.5 mL).
7. Centrifuge once again at 70,000 x g for 1 h at 4 °C, without brake (expect 1 h for deceleration). Carefully remove the supernatant without disturbing the pellet and leave 100 - 200 µL behind.
8. Resuspend the EV-pellet and adjust the final volume to 200 µL with PBS (standardized for all EV-isolations). Use the EV preparation immediately or store at -80 °C until use[22].
   NOTE: EVs can be stored up to 6 months at -80 °C.

2. EV Characterization.

Purified EVs can be visualized by transmission electron microscopy (TEM)[23].

1. Mix EV preps with an equal volume of 4 % paraformaldehyde in phosphate buffer.
2. Coat 200 mesh Formvar-carbon-coated nickel TEM grids with 5 µL of EV suspension for 20 min at room temperature.
3. Fixate the EV samples on TEM grids with 1 % glutaraldehyde in 0.1 M phosphate buffer (pH 7.0), contrast with uranyl oxalate (pH 7.0), and embed in a mixture of 4 % uranyl acetate and 2 % methyl cellulose in a 1:9 ratio on ice.
4. Remove grids with stainless steel loops and blot the excess fluid with filter paper to ensure an appropriate thickness of the methyl cellulose film.
5. After drying, examine grids with a transmission electron microscope and capture images with a digital camera coupled to the corresponding image software.

3. Education of MSCs by tumor-derived EVs.

1. Prepare MSC culture medium by supplementing alpha-minimum essential medium (alpha-MEM) with 4% EV-depleted human Platelet Lysate (hPL)[24], heparin (10 U/mL) and 1x P/S/G.
   NOTE: EV-depleted hPL is obtained following the procedure described in section 1.1.

2. Seed 1.4 x 10^6 adipose-derived MSCs per 75 cm^2 flask and culture them in EV-depleted MSC-culture medium in an incubator at 37 °C and 5% CO2.
3. When cells reach 70% confluence, add 143B osteosarcoma- or control human fibroblasts (hf)-EVs, 10 µL EV preparation/cm^2 of culture flask. Incubate for 24 hours and add the same amount of EVs for additional 6 hours. NOTE: Human fibroblasts are cultured in Dulbecco's Modified Eagle Medium (DMEM) 10% FBS and EVs are isolated as described in section 1.
4. Collect the MSC supernatant, centrifuge 1x at 500 x g for 5 min at 4 °C (with maximum acceleration and deceleration speed settings), transfer to a new tube and store the cleared supernatant at -80 °C to enable future cytokine analysis (section 5).
5. For *in vivo* experiments (section 6), educate GFP-positive MSCs[25] as described in sections 3.1 to 3.3, collect the cells and resuspend them in PBS at a final concentration of 10^6 cells per 100 µL. Keep cells on ice until injection.

4. EV Internalization Assay.

To visualize EV uptake by MSCs, label EVs with a green-fluorescent linker dye (GFLD) (commercially available) following the manufacturer's protocol:

1. Briefly, add 180 µL of diluent to the 200 µL EV prep. Dilute 1 µL of GFLD dye in 50 µL of diluent, and add 20 µL of diluted dye to the diluted EV prep.
2. Gently mix by pipetting and incubate for 3 min at room temperature in the dark.
3. Add 5 mL of 0.1 % BSA in PBS, transfer to ultra-centrifuge tubes and fill the tube with PBS (final volume 38.5 mL/tube).
4. Centrifuge 1x at 70,000 x g for 1 h at 4 °C, without brake (expect 1 h for deceleration). Carefully remove the supernatant and resuspend the labeled EV-pellet in a final volume of 200 µL (adjust volume with PBS).
5. Add the labeled EVs to the MSC culture or store them at -80 °C. After overnight incubation, assess vesicle internalization by fluorescence microscopy and flow cytometry[7].

5. Assessment of MSC Cytokine Expression Profile.

1. For the multiplex quantification of interleukin-8 (IL-8), interleukin-1β (IL-1β), interleukin-6 (IL-6), interleukin-10 (IL-10), tumor necrosis factor (TNF), and interleukin-12p70 (IL-12p70) protein levels in the MSC conditioned medium (see step 3.4), use a commercially available cytometric bead array (CBA) for human inflammatory cytokines following the manufacturer's instructions.
2. Briefly, mix the antibody-conjugated capture beads and add them to all assay tubes. Add the cytokine standard dilutions or the conditioned medium samples to the tubes.
3. Add the detection reagent and incubate 3 hours at RT.
4. Wash the beads with the supplied washing solution. Measure the samples using a flow cytometer and analyze the data according to the manufacturer's instructions.

6. Generation of an Orthotopic Xenograft Mouse Model of Osteosarcoma.

1. Allow six-week-old, female, Athymic Nude-Foxn1nu mice to acclimatize for at least one week before starting the experimental procedures.
2. One day before the surgical procedure and as peri-operative analgesia add paracetamol to the drinking water. Dilute "paracetamol solution for kids" (see **Table of Materials**) with water to get a final concentration of 2 mg/mL. Based on an average water intake of 150 mL/kg/day, and an average body weight of 20 g, this dose is sufficient to reach a dosage of 6 mg/mouse/day (300 mg/kg/day).
3. Continue analgesic treatment until 24 hours after the operation, or longer if the animals show signs of pain.
4. On the day of the surgical procedure, collect cultured luciferase-positive (Fluc) 143B cells (previously generated by lentiviral transduction) by centrifuging at 300 x g for 10 min and resuspend the cells at a concentration of 2 x 10^5 cells/µL in PBS. Keep the cell suspension on ice up to 6 hours.
5. Autoclave surgical equipment. Prepare and clean the working area and place the sterilized scissors and tweezers on sterile sheets. Twenty min before the surgical procedure (step 6.8), inject the animals subcutaneously with buprenorphine (0.05 mg/kg, diluted in 0.9% saline) as analgesic using 0.5 mL insulin syringes (29-gauge needle).
6. Just before anesthetizing each animal, fill a 10 µL syringe with at least 1 µL of the concentrated (Fluc) 143B cell suspension (see step 6.4).
7. Anesthetize the animal with isoflurane inhalation anesthesia (2 - 3% in oxygen). Check the level of anesthesia by toe-pinching the animal. When the animal does not react to the pinching, *i.e.,* it is deeply anesthetized, apply ointment on the eyes to prevent dryness during anesthesia.
8. Position the animal on its back with the head in an anesthesia mask and with the legs towards the operator. Flex the left knee. Wipe the skin with 70% ethanol and apply lidocaine (2%) with a cotton tip 3 times as local analgesic.
9. Use a sterile surgical knife to make a small incision (approximately 5 mm) on the skin just below the knee to expose the tibia. Drill a pinhole in the tibia, approximately 2 mm below the knee using a 0.8 mm micro twist drill. Be cautious not to drill through both tibia cortices.
10. Inject 1 µL cell suspension (approximately 2 x 10^5 cells) slowly (in approximately 5 seconds) into the hole using a 26-gauge needle. Close the hole with a droplet of tissue glue to prevent backflow of the suspension.
11. Close the skin with monofilament sutures and one drop of tissue glue. Let the animal recover in a well-heated environment (use a heat lamp). Do not leave animals unattended until they have regained sufficient consciousness to maintain sternal recumbency. Only after the animals are fully recovered from anesthesia, return them to their own cages.
12. Two days after tumor inoculation, inject EV educated or naïve GFP-positive MSCs (10^6 cells in 100 µL PBS, see step 3.5) intravenously with a 0.5 mL insulin syringe in the tail vein of the mice.
13. Follow tumor growth by bioluminescence imaging[26] twice a week. To this end, inject the mice i.p. with 150 µL D-luciferin (30 mg/mL) with an insulin syringe. Ten min after injection, position the animals in the bioluminescence imaging system and measure the photon-flux generated by tumor cells.
14. In addition, measure the diameter of the primary bone-tumor with a caliper. The tumor volume (in mm^3) is estimated by width x $length^2$ x 0.5.

15. NOTE: Humane endpoints are defined as tumor diameter >15 mm or weight loss >15%.

7. Assessment of Lung Nodule Number

1. When one of the animals reaches the humane endpoint defined in step 6.14 (in approximately 3 - 4 weeks), terminate the experiment and collect and analyze all relevant tissues.
2. Ten min before euthanization, inject 150 µL D-luciferin (30 mg/mL) with a 0.5 mL insulin syringe.
3. Anesthetize the animals with isoflurane inhalation anesthesia (see step 6.7). Confirm the depth of anesthesia by the absence of reactions of the mouse to toe-pinching. Euthanize the mice by cervical dislocation[27].
4. Collect lungs, liver, spleen and kidneys using sterilized scissors and tweezers. Wash the organs in PBS to remove blood traces and put them on a Petri dish.
5. Place the Petri dish with the organs in the bioluminescence imaging system. Measure the bioluminescence signal on both sides of the organs. Immediately after measuring, plunge the organs in 4% formalin to fixate them (24 - 72 hours, at RT) for future histological analysis.
6. Process the obtained pictures with appropriate imaging software by manual thresholding. Count the number of lung nodules on each picture. Count the total number of lung nodules on both sides of the lungs.

8. Histological Analysis

1. For histological analysis of the lung tissues:
    1. Embed the formalin-fixed organs in paraffin and prepare 6 µm tissue slides.
    2. Deparaffinate the lung tissue slides and perform antigen retrieval by boiling them for 15 min in 0.01 M citrate buffer (pH 6).
    3. Incubate the slides horizontally at room temperature with anti-human vimentin antibody (200 µg/mL) diluted 1:150 in antibody-diluent (commercially available) and subsequently with the secondary, HRP-labeled antibody (0.5 mg/mL, dilution 1:500). Stain the tissues with 3'-diaminobenzidine (DAB) and hematoxylin counter staining.
    4. Observe the stained tissue slides using an optical microscope coupled to the corresponding camera and image software.

2. To assess the presence of GFP-positive MSCs in mouse tibias:
    1. Decalcify the tibias in ethylenediaminetetraacetic acid (EDTA) 0.24 M, pH 7.2 - 7.4. Refresh EDTA buffer every other day until bones become flexible (approximately 1 week).
    2. Dehydrate tibias and infiltrate them with paraffin. Embed the tibias (including osteosarcoma tissue) in paraffin blocks.
    3. Use a microtome to prepare 6 µm paraffin sections. Place the paraffin sections onto glass slides. After drying, store slides overnight at room temperature.
    4. Perform heat-mediated antigen retrieval using citrate buffer (see 8.1.2) and stain the tissues with anti-GFP antibody (whole antiserum) in a 1:900 dilution in antibody-diluent. Counterstain the tissues with 4',6-diamidino-2-phenylindole (DAPI).
    5. Observe the tissue slides with a fluorescence microscope coupled to the corresponding imaging software.

Representative Results

In this study, we explored the ability of osteosarcoma-secreted EVs to educate MSCs towards a pro-tumorigenic and pro-metastatic phenotype. We show that osteosarcoma cells release exosome-like EVs that are internalized by MSCs. We measured the alteration of the MSC cytokine expression profile induced by cancer EVs, and evaluated the effect of the EV-educated MSCs on tumor growth and metastasis formation. The general representation of the study design is illustrated in **Figure 1**.

EVs released by 143B osteosarcoma cells or control human fibroblasts were purified by differential centrifugation. EV purity was confirmed by electron microscopy, which revealed that the preparations mainly contained vesicles with a diameter ranging between 40 - 100 nm (**Figure 2A**). To assess whether cancer EVs interact with MSCs, we labeled the vesicles with a green-fluorescent lipophilic linker dye (GFLD) and incubated them overnight with the target cells. By fluorescence microscopy we observed efficient EV uptake by MSCs (**Figure 2B**). Moreover, flow cytometry analysis showed that osteosarcoma and control EVs are internalized with comparable efficiency (**Figure 2C**). To investigate whether osteosarcoma EVs alter the immunomodulatory properties of MSCs, we used a multiplex bead-based cytokine immunoassay, which showed that tumor EVs determine a 2-fold increase in IL-8 and IL-6 production compared with human fibroblast control EVs (**Figure 2D,E**).

To investigate whether osteosarcoma EVs educate MSCs to adopt a pro-tumorigenic and pro-metastatic phenotype, we employed a bioluminescent, orthotopic xenograft mouse model of osteosarcoma. All animal experiments were performed by one operator. Metastatic 143B-Fluc cells were transplanted into the tibia of athymic nude mice, and, after two days, osteosarcoma-xenografted mice were subjected to a single administration of GFP-positive EV-educated MSCs. Mice receiving naïve (non-educated) MSCs or no MSCs were used as control groups. No animals died before the described endpoints. We demonstrated by caliper measurement and bioluminescence imaging (BLI) that mice treated with EV-educated MSCs had accelerated tumor growth compared with control groups (**Figure 3A**). Representative images of tumor size of each treatment arm are shown in **Figure 3C**. Our data indicate that a single i.v. administration of educated MSCs affects tumor progression as early as day 10 after inoculation (**Figure 3B**). In addition, four days after systemic injection of educated/naïve GFP-expressing MSCs (**Figure 4A**), we could visualize GFP-expressing cells both in the bone marrow (**Figure 4B**) and in the tumor tissue (**Figure 4C**), demonstrating MSC homing to the tumor site.

Ex vivo BLI analysis of lungs, liver, kidney and spleen (data not shown) showed lung nodule formation exclusively in the lungs in mice of all treatment arms (**Figure 4D-F**). Strikingly, mice receiving EV-educated MSCs had higher number of lung metastases compared with mice receiving non-educated MSCs or no MSCs (**Figure 4G**), suggesting that within the tumor microenvironment educated MSCs increase the metastatic potential of osteosarcoma cells *in vivo*[7].

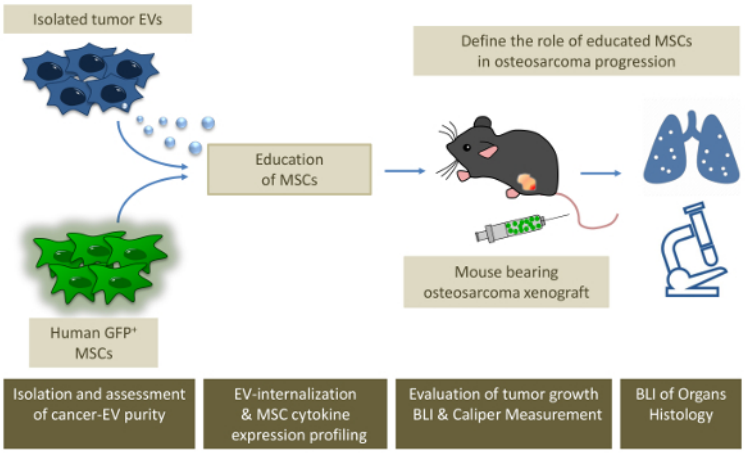

Figure 1. Schematic representation of the study design. Human primary MSCs are educated with EVs isolated from cultured metastatic osteosarcoma (143B) cells. Cancer EV purity is assessed by electron microscopy, and internalization by MSCs is visualized by fluorescence microscopy and analyzed by flow cytometry. Changes in the MSC cytokine expression profile are evaluated by cytometric bead array (CBA). To define the role of EV educated MSC on tumor growth and metastasis formation, osteosarcoma-bearing mice are injected with EV-educated (or naïve) MSC. Tumor growth is followed by bioluminescence imaging (BLI) and caliper measurement, while metastasis formation is evaluated at the experimental end-point by *ex vivo* BLI and histological analysis. Please click here to view a larger version of this figure.

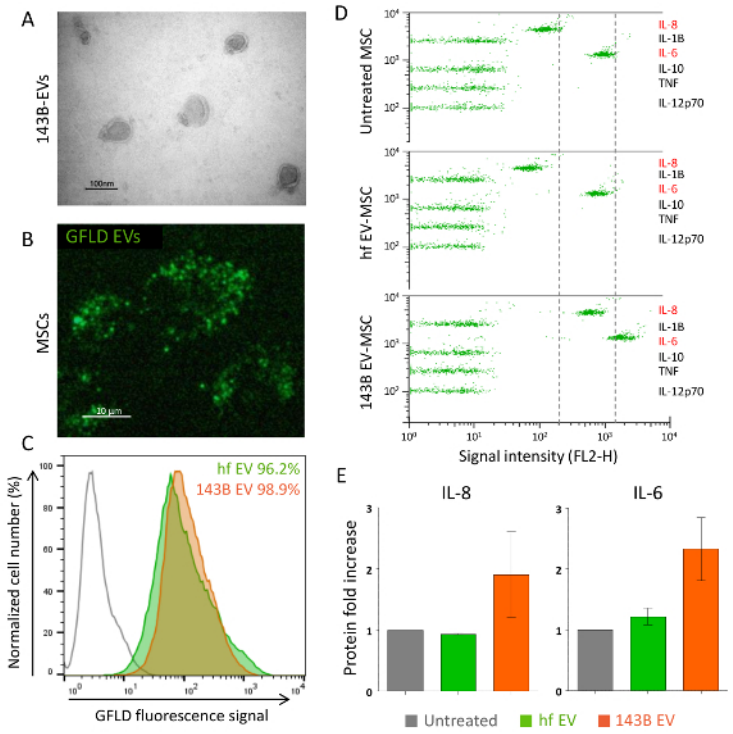

Figure 2. Purification of EVs and their interaction with MSCs. (A) Transmission electron microscopy micrograph of EVs isolated from 143B cells (scale bar: 100 nm). **(B)** Uptake of GFLD-labeled 143B EVs by MSCs assessed by fluorescence microscopy (scale bar: 10 µm). **(C)** Internalization of GFLD-labeled 143B EVs (orange) or control (human fibroblast, hf) EVs (green) by MSCs as analyzed by flow cytometry. **(D)** Multiplex detection of inflammatory cytokines in the supernatants of MSCs exposed to 143B (143B EV-MSC) or hf-EVs (hf EV-MSC) by cytometric bead array. 143B-MSC express higher levels of IL-6 and IL-8 compared to control (untreated and hF EV-treated) MSCs. The dotted lines indicate the shift in cytokine production. **(E)** IL-8 and IL-6 protein concentration in the conditioned media of EV-treated MSCs as analyzed by cytometric bead array, expressed as fold induction relative to the untreated control. Data are expressed as mean ± SD, n = 2. Please click here to view a larger version of this figure.

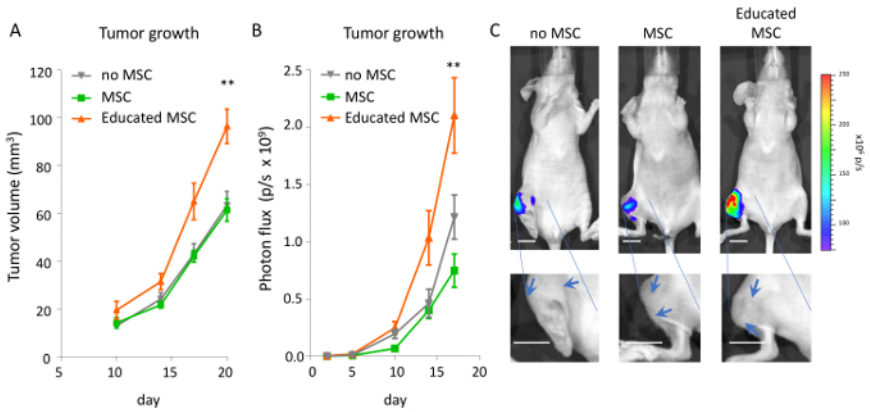

Figure 3. Bioluminescent, orthotopic xenograft mouse model of osteosarcoma. (A) Estimation of tumor volume using caliper measurements, and **(B)** tumor growth measured by bioluminescence imaging (BLI). Tumor size is expressed as photon flux (photons/sec). ** $p < 0.01$, non-educated MSC (n=6) *vs* educated MSC (n = 6), unpaired t-test. Data are expressed as mean ± SEM. **(C)** Representative BLI images of mice with established osteosarcoma tumors (top panel). Color-scale bar ranges from 7.7 x 10^7 (purple) to 2.6 x 10^8 (red) photons/sec. In the bottom panel, the tumor area is visualized without BLI overlay. Arrows indicate the tumor bulk. Scale bars: 0.6 cm. Please click here to view a larger version of this figure.

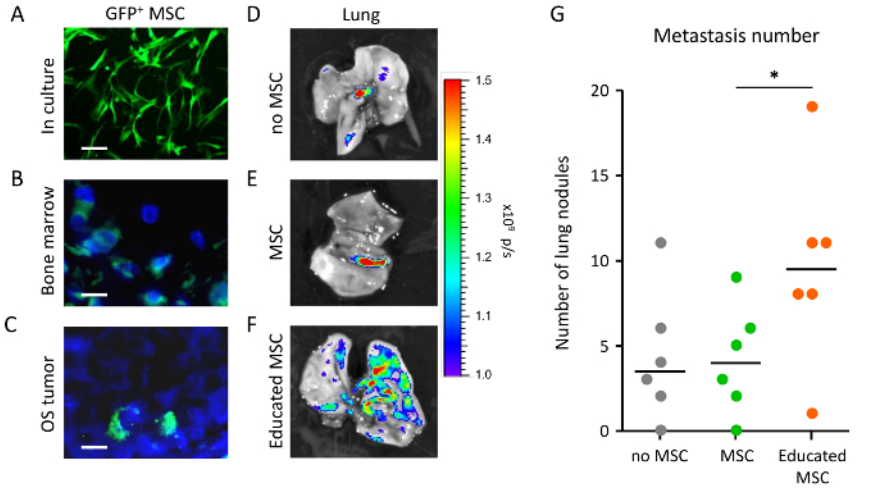

Figure 4. Imaging of MSCs and *ex vivo* lung tissue. (A) Fluorescence microscopy image of cultured GFP-positive adipose-derived MSCs (green). **(B)** Immunofluorescence staining of GFP-positive MSCs in the bone marrow and **(C)** in tumor tissue of MSC-receiving mice (green: MSCs, blue: DAPI stained nuclei; scale bar 10 µm). **(D-F)** *Ex vivo* bioluminescence imaging (BLI) showing higher number of metastatic foci in mice receiving EV-educated MSCs **(F)** as compared to mice receiving naïve MSC **(E)** or no MSC **(D)**. Color scale bar ranges from 1 x 10^6 (purple) to 1.5 x 10^6 (red) photons/sec**. (G)** Quantification of lung metastasis number as visualized by BLI (Lines represent the median; * $p < 0.05$, one-tailed t-test). Please click here to view a larger version of this figure.

Discussion

Tumor-secreted extracellular vesicles (EVs) can alter the physiology of local and distant mesenchymal cells to generate a tumor-supportive environment. Here we describe the generation of a preclinical mouse model of osteosarcoma that allows dissection of the EV-mediated interactions between tumor cells and mesenchymal stem cells (MSCs) *in vivo*. We show that systemic injection of human tumor EV-educated MSCs in mice bearing osteosarcoma xenografts strongly promotes cancer growth and metastasis formation by activating the IL-6/STAT3 signaling pathway[7].

Recent studies have shown that cancer EVs can aid in the formation of the pre-metastatic niche by altering the behavior of local or bone marrow-derived stromal cells[16,28,29]. These studies have been mostly conducted by directly injecting cancer-derived vesicles in the recipient mouse, which complicates the identification of the cell types responsible for the tumor-promoting effects. In our protocol, the education of MSCs with cancer EVs occurs *in vitro* prior to MSC injection. This approach allows addressing of the specific contribution of the tumor-MSC crosstalk to cancer progression, and minimizes confounding indirect effects of cancer EVs on other components of the local or systemic environment.

To evaluate whether the educated MSCs home to the tumor site, we systemically injected GFP-positive MSCs in the tail vein of the tumor-bearing mice. Tail vein injections are a crucial, but technically challenging step in many experimental protocols. To ensure minimal variation among injections the procedure should be performed by experienced investigators. Correct intravenous administration can be visually confirmed by observing the movement of the fluid through the vein. If a white area appears on the tail or resistance is encountered during injection, vascular

access was not achieved. In this case the procedure should be repeated by inserting the needle above the first injection site. Because MSCs readily home in on the tumor, successful administration of (GFP-positive) MSCs can be confirmed by immunofluorescence staining of the tumor tissue and bone marrow four days after injection (**Figure 4B,C**).

We show that cancer-secreted EVs induce a tumor-supportive phenotype in MSCs by altering the production of inflammatory cytokines. This finding is particularly relevant since immune modulation and tumor immune evasion are key mechanisms in malignant progression. Our data suggest that cancer EVs might directly, as reported by independent studies[21,30,31,32,33], or indirectly (via MSCs) influence innate or adaptive immune components. However, the use of a xenograft (immunocompromised) model limits the possibility to investigate this aspect of EVs. Thus, similar approaches in immunocompetent or humanized mouse models need to be undertaken to define the role of the EV-mediated tumor-MSC-immune cell interactions in cancer.

Finally, because MSCs can be recruited from the bone marrow or other tissue sources to tumors, our method is not restricted to the study of bone cancers, but can be applied to investigate the role of tumor EV-educated MSCs in multiple cancer types[2,3,4,5,6], as recent studies in melanoma and lymphoma models confirm[34].

Disclosures

The authors have nothing to disclose.

Acknowledgements

S.R. Baglio was supported by a fellowship by Associazione Italiana per la Ricerca sul Cancro (AIRC) co-funded by the European Union,. In addition, this project has received funding from the European Union's Horizon 2020 research and innovation programme under the Marie Sklodowska-Curie grant agreement No 660200 (to S.R. Baglio).

References

1. Hanahan, D., Weinberg, R. A. Hallmarks of cancer: The next generation. *Cell.* **144** (5), 646-74 (2011).
2. Karnoub, A. E. *et al.* Mesenchymal stem cells within tumour stroma promote breast cancer metastasis. *Nature.* **449** (7162), 557-563 (2007).
3. Jung, Y. *et al.* Recruitment of mesenchymal stem cells into prostate tumours promotes metastasis. *Nat Commun.* **4**, 1795 (2013).
4. Shahar, T. *et al.* Percentage of mesenchymal stem cells in high-grade glioma tumor samples correlates with patient survival. *Neuro Oncol.* **19** (5), now239 (2016).
5. Behnan, J. *et al.* Recruited brain tumor-derived mesenchymal stem cells contribute to brain tumor progression. *Stem Cells.* **32** (5), 1110-23 (2014).
6. Giallongo, C. *et al.* Granulocyte-like myeloid derived suppressor cells (G-MDSC) are increased in multiple myeloma and are driven by dysfunctional mesenchymal stem cells (MSC). *Oncotarget.* **7** (52), 85764-85775 (2016).
7. Baglio, S. R. *et al.* Blocking tumor-educated MSC paracrine activity halts osteosarcoma progression. *Clin Cancer Res.* **23**(14):3721-3733 (2017).
8. Pittenger, M. F. *et al.*Multilineage potential of adult human mesenchymal stem cells. *Science.* **284** (5411), 143-7 (1999).
9. Shi, Y., Du, L., Lin, L., Wang, Y. Tumour-associated mesenchymal stem/stromal cells: emerging therapeutic targets. *Nat Rev Drug Discov.* **16** (1), 35-52 (2017).
10. Ridge, S. M., Sullivan, F. J., Glynn, S. A. Mesenchymal stem cells: key players in cancer progression. *Mol Cancer.* **16** (1), 31 (2017).
11. Luo, J. *et al.* Infiltrating bone marrow mesenchymal stem cells increase prostate cancer stem cell population and metastatic ability via secreting cytokines to suppress androgen receptor signaling. *Oncogene.* **33** (21), 2768-2778 (2013).
12. Huang, W.-H., Chang, M.-C., Tsai, K.-S., Hung, M.-C., Chen, H.-L., Hung, S.-C. Mesenchymal stem cells promote growth and angiogenesis of tumors in mice. *Oncogene.* **32** (37), 4343-54 (2013).
13. Patel, S. A., Meyer, J. R., Greco, S. J., Corcoran, K. E., Bryan, M., Rameshwar, P. Mesenchymal stem cells protect breast cancer cells through regulatory T cells: role of mesenchymal stem cell-derived TGF-beta. *J Immunol.* **184** (10), 5885-94 (2010).
14. Becker, A., Thakur, B. K., Weiss, J. M., Kim, H. S., Peinado, H., Lyden, D. Extracellular vesicles in cancer: Cell-to-cell mediators of metastasis. *Cancer Cell.* **30** (6), 836-848 (2016).
15. Skog, J. *et al.* Glioblastoma microvesicles transport RNA and protein that promote tumor growth and provide diagnostic biomarkers. *Nat Cell Biol.* **10** (12):1470-6 (2008).
16. Peinado, H. *et al.* Melanoma exosomes educate bone marrow progenitor cells toward a pro-metastatic phenotype through MET. *Nat Med.* **18** (6), 883-91 (2012).
17. Zomer, A. *et al.* In vivo imaging reveals extracellular vesicle-mediated phenocopying of metastatic behavior. *Cell.* **161** (5), 1046-1057 (2015).
18. Webber, J., Steadman, R., Mason, M. D., Tabi, Z., Clayton, A. Cancer exosomes trigger fibroblast to myofibroblast differentiation. *Cancer Res.* **70** (23), 9621-30 (2010).
19. Webber, J. P. *et al.* Differentiation of tumour-promoting stromal myofibroblasts by cancer exosomes. *Oncogene.* **34** (3), 290-302 (2015).
20. Zhou, W. *et al.* Cancer-secreted miR-105 destroys vascular endothelial barriers to promote metastasis. *Cancer Cell.* **25** (4), 501-515 (2014).
21. Whiteside, T., Anastasopoulou, E., Voutsas, I., Papamichail, M., Perez, S., Nunes, D. Exosomes and tumor-mediated immune suppression. *Expert Rev Mol Diagn.* **15** (10), 1293-1310 (2016).
22. Verweij, F. J., Van Eijndhoven, M. A. J., Middeldorp, J., Pegtel, D. M. Analysis of viral microRNA exchange via exosomes in vitro and in vivo. *Methods Mol Biol.* **1024**, 53-68 (2013).
23. Baglio, S. R. *et al.* Human bone marrow- and adipose-mesenchymal stem cells secrete exosomes enriched in distinctive miRNA and tRNA species. *Stem Cell Res Ther.* **6** (1), 127, (2015).
24. Naaijkens, B. A. *et al.* Human platelet lysate as a fetal bovine serum substitute improves human adipose-derived stromal cell culture for future cardiac repair applications. *Cell Tissue Res.* **348** (1), 119-30 (2012).

25. Grisendi, G. *et al.*Adipose-derived mesenchymal stem cells as stable source of tumor necrosis factor-related apoptosis-inducing ligand delivery for cancer therapy. *Cancer Res.* **70** (9), 3718-29 (2010).
26. Cosette, J., Abdelwahed, R. Ben, Donnou-Triffault, S., Sautès-Fridman, C., Flaud, P., Fisson, S. Bioluminescence-based tumor quantification method for monitoring tumor progression and treatment effects in mouse lymphoma models. *J Vis Exp.* (113) (2016).
27. Carbone, L. *et al.* Assessing cervical dislocation as a humane euthanasia method in mice. *J Am Assoc Lab Anim Sci.* **51** (3), 352-6 (2012).
28. Costa-Silva, B. *et al.*Pancreatic cancer exosomes initiate pre-metastatic niche formation in the liver. *Nat Cell Biol.* **17** (6), 816-826 (2015).
29. Hoshino, A. *et al.* Tumour exosome integrins determine organotropic metastasis. *Nature.* **527** (7578), 329-35 (2015).
30. Clayton, A., Mitchell, J. P., Court, J., Mason, M. D., Tabi, Z. Human tumor-derived exosomes selectively impair lymphocyte responses to interleukin-2. *Cancer Res.* **67** (15), 7458-7466 (2007).
31. Wieckowski, E. U., Visus, C., Szajnik, M., Szczepanski, M. J., Storkus, W. J., Whiteside, T. L. Tumor-derived microvesicles promote regulatory t cell expansion and induce apoptosis in tumor-reactive activated cd8+ T lymphocytes. *J Immunol.* **183** (6), 3720-3730 (2009).
32. Valenti, R., Huber, V., Iero, M., Filipazzi, P., Parmiani, G., Rivoltini, L. Tumor-released microvesicles as vehicles of immunosuppression. *Cancer Res.* **67** (7), 2912-2915 (2007).
33. Costa-Silva, B. *et al.* Pancreatic cancer exosomes initiate pre-metastatic niche formation in the liver. *Nat Cell Biol.* **17** (6), 816-826 (2015).
34. Lin, L. Y. *et al.*Tumour cell-derived exosomes endow mesenchymal stromal cells with tumour-promotion capabilities. *Oncogene.* **35** (46), 6038-6042 (2016).

